ISBN: 978-3-95450-199-1 doi:10.18429/JACoW-SAP2017-MOBH1

EXPERIMENTAL STUDY ON THE ELECTRON SUPERCONDUCTING LINAC AND ITS APPLICATION*

Kexin Liu†, Shengwen Quan, Jiankui Hao, Senlin Huang, Lin Lin,
Liwen Feng, Fang Wang, Feng Zhu, Huamu Xie, Limin Yang, Jia-er Chen
Institute of Heavy Ion Physics & State Key Laboratory of Nuclear Physics and Technology
Physics and Technology, Peking University, Beijing, China

Abstract

Experimental study on superconducting electron linac has been developed at Peking University. Stable operation of a DC-SRF photoinjector and a 2×9-cell SRF linac has been realized with an average beam current of mA scale in macro pulses of several ms with a repetition rate of 10 Hz. A compact high repetition rate THz radiation source has been developed based on DC-SRF photo-injector through velocity bunching. Superradiant THz radiation with a repetition rate of 16.25 MHz and a frequency that can be tuned from 0.24 to 0.42 THz was generated by varying the electron beam energy from 2.4 to 3.1 MeV. MeV UED at MHz repetition rate has been demonstrated experimentally using electron pulses from the DC-SRF photoinjector. THz undulator radiation of ~1 THz central frequency with an average power of 1 W has been achieved with 13 MeV electron beam from SRF linac and applications are underway.

INTRODUCTION

To obtain electron beams with high average current and low emittance, superconducting radiofrequency (SRF) photocathode guns, which combine the high brightness of normal conducting RF photocathode guns with the advantage of CW operation of superconducting RF cavities, have been developed in many laboratories worldwide [1, 2].

DC-SRF photoinjector, which combines a DC Pierce gun and a superconducting cavity, was first proposed by Peking University in 2001 [3] and demonstrated with a 1.5-cell TESLA type superconducting cavity in 2004 [4]. An upgraded DC-SRF injector with a 3.5-cell large grain niobium cavity was then designed and constructed [5]. Electron beam with a current of mA level has been obtained at long-term stable operation. At the same time, a 1.3 GHz superconducting linac containing two 9-cell cavities was designed, setup and commissioned. Electron beam of 8-25 MeV was obtained by combination of the DC-SRF photoinjector and SRF linac.

Some applications with superconducting electron linac have been carried out at Peking University. Based on the DC-SRF photoinjector, a compact THz radiation source through velocity bunching was constructed to generate THz pulses with a high repletion rate. MeV ultrafast electron diffraction (UED) at MHz repetition rate has been demonstrated experimentally using electron pulses from the DC-SRF photoinjector. With 13 MeV electron beam from SRF linac, THz undulator radiation are generated and an average power of 1 W in macro pulse has been achieved.

In this paper, the experimental studies on DC-SRF photoinjector and superconducting linac, the applications with electron beam from superconducting injector and linac are reported.

STUDY ON DC-SRF PHOTOINJECTOR

DC-SRF Photoinjector

Figure 1 shows the schematic view of the upgraded DC-SRF photoinjector, which consists of the DC pierce gun, 3.5-cell SRF cavity, helium vessel, liquid nitrogen shield, input power coupler, tuner and auxiliary systems.

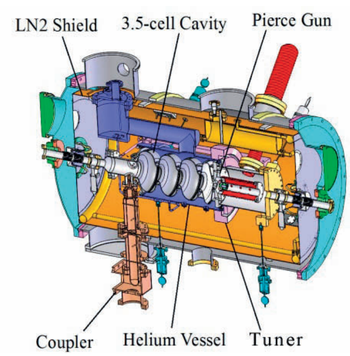

Figure 1: Schematic view of the DC-SRF photoinjector.

The designed DC voltage of Pierce gun is 90 kV. The surface electric field on the cathode is almost 5 MV/m and the peak electric field is lower than 13 MV/m. The 3.5-cell large grain niobium superconducting cavity comprises three TESLA type cells and a special designed half-cell. The accelerating gradient of the cavity reaches 23.5 MV/m and the intrinsic quality factor Q_0 is higher than 1.2×10^{10} in vertical test [5]. The input power coupler adopts compact capacitive coupling structure [6].

Cs_2Te photocathode is used for DC-SRF injector. The upgraded drive laser system composes of a Time-Bandwidth GE-100 XHP seed laser, amplifier, second harmonic generator, fourth harmonic generator and optical beam line to transport the UV pulses to the photocathode. The repetition rate of laser pulses is 81.25 MHz. The drive laser system can provide 1 W power in a train of 6 ps UV (266 nm) pulses with 5% power instability. The deposition of photocathode is accomplished in the vacuum of about 1.2×10^{-8} mbar. The Cs_2Te cathode is activated again with cesium just before

*Work supported by National Key Programme for S&T Research and Development (Grant NO.:2016YFA0401904)
† kxliu@pku.edu.cn

ISBN: 978-3-95450-199-1 doi:10.18429/JACoW-SAP2017-MOBH1

transferring it into the cryomodule. Quantum efficiency (QE) and life time of the cathode have been improved obviously after reactivation. The QE was more than 10% at the beginning and then stabilized at about 4% for more than 10 days. After one more week, the photocathode was illuminated again by drive laser and the QE was still 2% and lasted for a long time.

In order to stabilize the accelerating field of the 3.5-cell SRF cavity, a digital LLRF control system was designed. By comparing the pick-up signal with the set point, the PI controller in FPGA can adjust output signal to compensate the deviation, thus maintain stable field in the cavity [7]. To allow pulse operation, gate signal has been added to the feedback loop and the control algorithm has been modified to handle Lorentz force detuning.

A diagnostic beam line is designed and constructed, as shown in Fig. 2. Two solenoid lenses, a quadrupole magnet and a dipole magnet are adopted for beam focusing and deflecting. The first solenoid lens is installed as close as possible to the cryomodule for emittance compensation. The dipole magnet is used to deflect the electron beam to a Faraday cup with water cooling as dump. Beam diagnostic devices including YAG screen, Faraday cups and a beam emittance meter are installed in beam line.

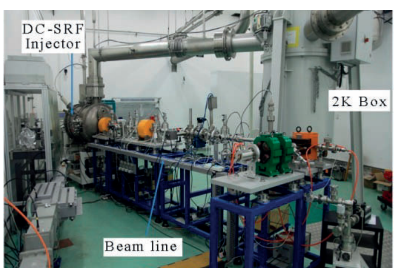

Figure 2: Beam line of the 3.5-cell DC-SRF injector.

RF and Beam Experiments

The E_{acc} of 3.5-cell cavity reached 14.5 MV/m in CW mode and 17.5 MV/m in pulsed mode with a duty factor of 10% and a repetition rate of 10 Hz. The amplitude (up) and phase (below) signals of 3.5-cell DC-SRF injector without beam load is shown in Fig. 3. The instability is less than 0.1% for amplitude and 0.1 degree for RF phase.

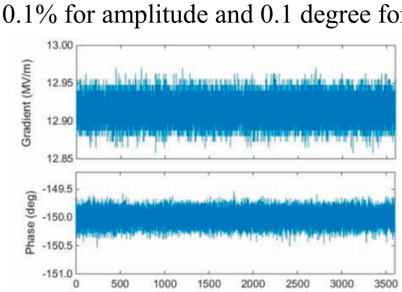

Figure 3: Long-term running of LLRF control system.

The beam experiments were carried out at E_{acc} of 8.5 MV/m for stable operation and at a low average current in order to avoid electron beam bombarding the beam tube. We reduced the duty factor of drive laser instead of the laser pulse energy to keep the same bunch charge for different average current. The average beam current was about 2.5 μA when the duty factor of the drive laser was 1% at a repetition rate of 10 Hz. The duty factor was then increased to 100% gradually and the average current increased to 250 μA at CW mode operation. The beam current was increased further by increasing laser power, but the degassing of the dump Faraday cup became serious. Pulsed mode was applied for long term beam test to protect the superconducting cavity. The duty factor of RF power was 7% with a repetition rate of 10 Hz. The average beam current in a macro pulse reached 1 mA and was kept at 0.55 mA for long term operation.

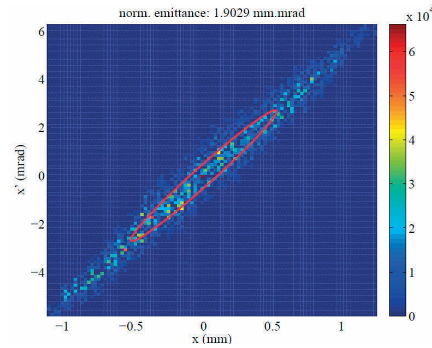

Figure 4: measured emittance of electron beam.

The kinetic energy of electron beam of 3.4 MeV was measured with the bending magnet. This was consistent with the value derived from the accelerating gradient. The measured normalized emittance was about 1.9 mm·mrad, see Fig. 4. More simulation work is underway to reduce the emittance of the DC-SRF photoinjector.

APPLICATIONS OF DC-SRF PHOTOINJECTOR

Superradiant THz Undulator Radiation

Based on the DC-SRF photoinjector, we constructed a compact THz radiation source through velocity bunching to generate THz pulses with a high repetition rate, see Fig. 5. A solenoid, following the DC-SRF photo-injector, is used to focus the electron beam and compensate emittance growth. A 10-period planar undulator is installed 6.0 m downstream of the photocathode. Velocity bunching [8, 9] by the rf field of the superconducting cavity is applied to compress electron bunches. Between the solenoid and the undulator are only several pairs of steering coils. A dipole magnet is placed after the undulator to bend the electron beam to a dump.

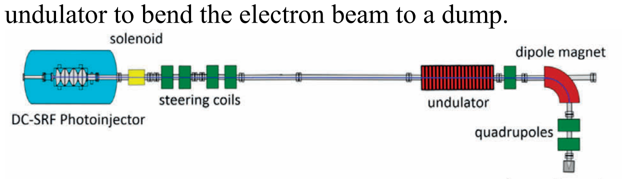

Figure 5: Layout of the compact THz system at PKU.

The simulated longitudinal distribution of electrons was obtained using the tracking code ASTRA. In the simulation, the space charge effect was taken into account

ISBN: 978-3-95450-199-1 doi:10.18429/JACoW-SAP2017-MOBH1

and the wake field effect was not implemented due to the low beam peak current. The electron beam parameters used for the simulation, as well as the undulator parameters, are listed in Table 1. To determine the maximum THz radiation power, we investigated electron distribution at the undulator entrance in the longitudinal phase space under different rf phases of 0° to −40°. Here, 0° is defined as the on-crest acceleration phase. For each phase, the solenoid magnetic field was adjusted to focus the electron beam to form a waist at the undulator center. The longitudinal position of the electrons was derived from the ASTRA output, and the coherent enhancement factor F_{ce} was obtained. A maximum coherent enhancement factor of 4.3×10^{6} was obtained at an acceleration phase of −24°. The corresponding electron distribution in the longitudinal phase space and the current profile of the electron bunches are shown in Fig. 6. This asymmetric current profile with a sharp peak in the tail confers high F_{ce} because some electrons are squeezed into a very narrow region.

Table 1: Operation Parameters of DC-SRF Photo Injector

Parameter	Value
Electron beam at photocathode	
Beam size (rms)	1.0 mm
Bunch length (FWHM)	5 ps
Repetition rate	16.25 MHz
Bunch charge	25 pC
Undulator	
Number of Periods	10
Period length λ_u	27 mm
rms strength parameter a_u	**1**

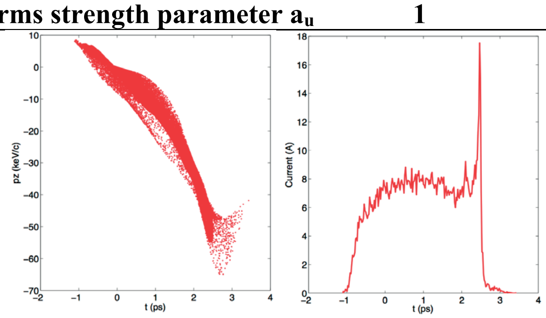

Figure 6: Electron distribution in the longitudinal phase space (left) and the current profile of electron bunches (right) at the undulator entrance when the rf phase is −24°.

The calculated maximum power of the superradiant THz radiation from the undulator is ~1 W. The maximum THz power obtained at the exit of the dipole magnet chamber is 5.7 mW if the propagation loss is considered.

Figure 7 shows the experimental setup for THz radiation power and spectrum measurement, which is composed of two off-axis parabolic reflecting mirrors, two identical z-cut quartz windows with a transparency of 70% each, a Fourier transform far-infrared spectrometer (FTS) for spectrum measurement, and a Golay cell detector for radiation power measurement. An attenuator is installed before the Golay cell to avoid saturation. THz radiation is transported in vacuum (100 Pa) to reduce THz absorption by water vapor and CO2.

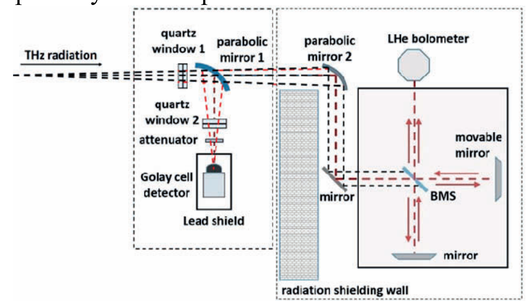

Figure 7: Schematic of the THz measurement system.

The production and measurement of THz is straight forward. The photoinjector was operated in macro pulse mode for safe operation. The macro pulse repetition rate is 7 Hz, and the duty factor is 2.8%. Accelerating gradients were varied to generate THz radiation with different central wavelengths. For each accelerating gradient, the solenoid and steering coils were optimized to ensure effective electron beam transport in the vacuum chamber of the undulator. The accelerating phase was also adjusted to obtain the maximum THz radiation power.

The measured THz radiation spectra are shown in Fig. 8. The central frequency ranges from 0.24 THz to 0.42 THz when electron beam energy varies from 2.4 to 3.1 MeV, and the FWHM bandwidth is approximately 0.05 THz. Electron beam transport is more difficult at electron beam energy lower than 2.4 MeV.

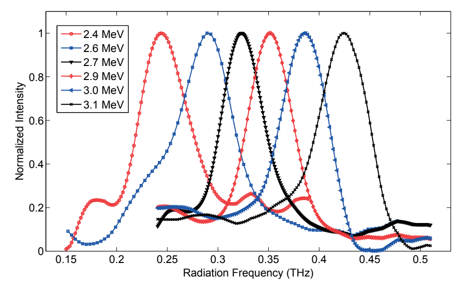

Figure 8: Measured THz spectra with different electron beam energies.

THz radiation power was measured at different rf phases of the SRF cavity with an interval of 5°. Fig. 9 shows the measured THz radiation power and the calculated results, wherein propagation losses were considered. The power at mW level in macro pulses was obtained at about −25°. The figure shows good agreement between calculation and experimental measurements.

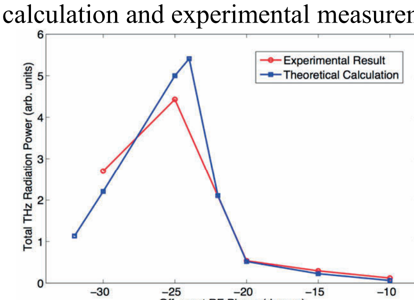

Figure 9: Measured and calculated THz power at different rf phases.

ISBN: 978-3-95450-199-1 doi:10.18429/JACoW-SAP2017-MOBH1

The total superradiant radiation power is evaluated to be about 5.65 mW, which comprises 4.76 mW (84%) fundamental radiation and 0.89 mW (16%) higher-order harmonic radiation. The fundamental radiation contributes more than 80% to the measured mW level THz radiation power.

MHz MeV UED

The first MeV UED that operates at the MHz repetition rate regime was carried with electron beams from DC-SRF photoinjector. The layout of the MHz MeV UED proof-of-principle experiment is shown in Fig. 10.

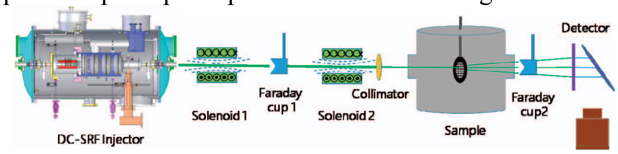

Figure 10: Schematic layout of the MeV MHz UED beam line.

The MHz MeV pulsed electron beam is produced with DC-SRF photoinjector. The repetition rate of the electron beam can be varied from 162.5 kHz up to 81.25 MHz and the average beam current can be varied from about 1 nA up to 1 mA by changing the laser power and laser repetition rate. The electron pulse length is expected to be about 5 ps (FWHM), which is limited by the pulse length of the photocathode drive laser. By running the electron beam at off-crest phase in the superconducting rf cavities, the electron pulse can be significantly shorter than the laser pulse due to velocity bunching.

After exiting the injector, the beam is focused by a solenoid to maintain a reasonable beam size during the transportation to the UED beam line. Then a second solenoid is used to minimize the beam size at the phosphor screen to maximize the contrast of the diffraction pattern. A collimator with 2 mm diameter is put upstream of the sample chamber to remove beam halo that would otherwise contribute to a large background to the diffraction pattern. Both single crystalline Au and polycrystalline Al samples were used in the experiments, which were mounted on a motorized stage in the sample chamber. The detector was composed of a phosphor screen, located at 2.6 m downstream of the sample, a 45° mirror, and a high-efficiency CCD camera. The average beam current at the exit of the photoinjector and at the exit of the sample can be measured with Faraday cups.

Figure 11 shows the measured diffraction patterns for a 20 nm thick single-crystal Au foil and a polycrystalline Al foil. The diffraction pattern was obtained by integrating the signal over 200 ms when the beam repetition rate is 812.5 kHz. The total beam charge (after the sample) for Fig. 11 is measured to be about 33 pC, corresponding to about 0.2 fC per pulse. To protect the phosphor screen and the sample, we intentionally lowered the drive laser energy and repetition rate to reduce the number of electrons passing through the sample.

The projection of the diffraction spots taken along the line indicated in Fig. 11a is shown in Fig. 11c. All spots including the direct beam have approximately the same width which is found to be about 0.1 A^{-1} (FWHM), implying good spatial coherence of the beam. To quantify the spatial coherence of the beam, we compared the sharpness of the diffraction spots with that calculated from multi-slit interference [10, 11] where the half angle spread is related to the beam transverse coherence as $\Delta\theta=\lambda/Nd$, where N is the number of slits in the coherently illuminated area and d is the distance of the slits. With the spot width being about 0.7 mm (FWHM), the spatial coherence of the beam is estimated to be about 1.5 nm. With the diffraction angle being $\theta=\lambda(k^2+l^2+m^2)^{1/2}/a_0$, where λ is the De Broglie wavelength, k, l, m are the Miller indices and a_0 is the lattice constant, the electron De Broglie wavelength is determined to be about 0.42 pm and the corresponding beam energy is quantified to be about 3.0 MeV, in good agreement with that measured with an energy spectrometer.

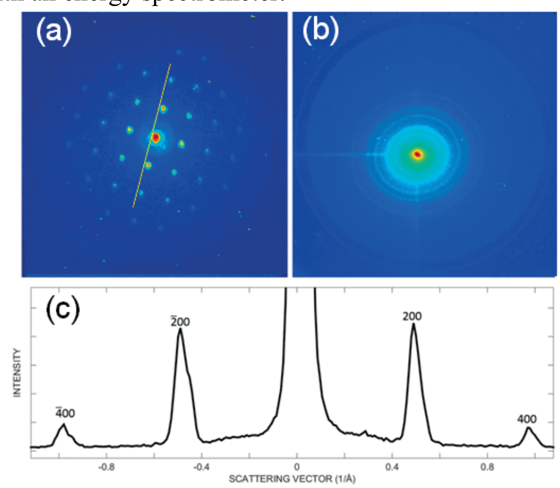

Figure 11: Measured electron diffraction patterns from a single-crystalline Au foil (a) and a polycrystalline Al foil (b) taken at 812.5 kHz repetition rate with an integration time of 200 ms; (c) Intensity projections along the (200) and (400) spots in (a).

STUDY AND APPLICATION OF 2×9-CELL SRF LINAC

Commissioning of 2×9-cell SRF Linac

To improve the energy of electron beam, a main SRF linac is designed and constructed, which contains two 9-cell TESLA cavities, input power couplers, frequency tuners, helium vessel, liquid nitrogen shield, magnetic shield and its associated auxiliary systems. Fig. 12 gives the sectional view of the 2×9-cell linac.

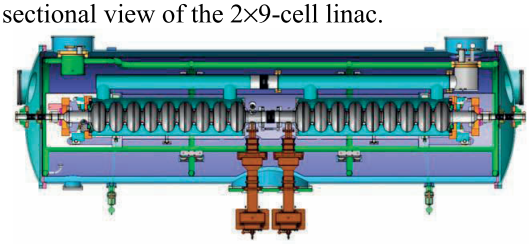

Figure 12: The sectional view of 2×9-cell SRF linac.

ISBN: 978-3-95450-199-1 doi:10.18429/JACoW-SAP2017-MOBH1

Both 9-cell cavities (PKU2 and PKU4) are made from Ningxia large grain niobium material and fabricated by PKU. The accelerating gradients in vertical test are 22.4 MV/m for PKU2 and 32.6 MV/m for PKU4. Quality factor of both cavities are higher than 1×10^{10} at the quench gradients.

An improved LLRF system was designed and setup for SRF linac. A compact LO/Digital clock generation board using commercial PLL ICs was developed. A Digital Phase Lock Loop (DPLL) based reference racking algorithm was developed to cancel the LO/Digital clock noise. Stability of the upgraded LLRF system is 0.01% for amplitude and 0.02° for phase.

Commissioning of SRF linac was finished in Oct. 2015. Due to the capacity limit of the cryogenic system, the SRF linac can only run at long macro pulse mode. The accelerating gradient of both cavities in horizontal test are ~20 MV/m. Electron beam loading test was carried out by combination of DC-SRF photoinjector and SRF linac. An average current of ~1 mA was obtained with macro pulse duration of 5 ms and duty factor of 5%.

THz Undulator Radiation with SRF Linac

Based on the stable operation of DC-SRF photo-injector and SRF linac, THz undulator radiation experiments are carried out with high repetition rate ~15 MeV electron beam. The layout of the THz system is shown in Fig. 13. A Chicane structure is installed after the SRF linac for further electron bunch compression. An upgraded 10-period undulator with tuneable gap is installed downstream of the Chicane. FTS and Golay cell detector are used for spectrum and radiation power measurements.

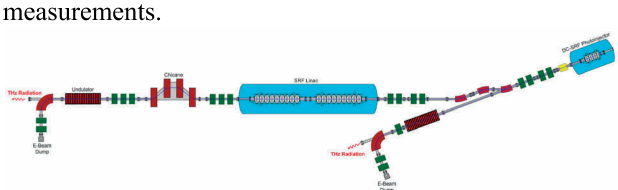

Figure 13: Layout of the compact THz system at PKU.

The coherent enhancement factor F_{ce} was obtained with the longitudinal position of the electrons derived from the ASTRA output. Coherent enhancement factor is 2×10^7 at 350 μm central wavelength with electron beam of 14 MeV energy, 450 μA average current and 27 MHz repetition rate, when the undulator gap is 10 mm.

The measured THz radiation spectra with different electron beam energies and undulator gaps are shown in Fig. 14. The central frequency ranges from 0.83 THz to 1.02 THz with fixed gap of 10 cm when the electron beam energy varies from 11.4 MeV to 12.6 MeV. With fixed electron beam energy of 11.4 MeV, the central frequency changes from 0.92 THz to 1.28 THz when the gap varies from 10 mm to 12 mm. The FWHM bandwidth is approximately 0.1 THz.

THz radiation power was measured at macro pulse length of 2 ms, duty cycle of 1% and macro pulse length of 7 ms, duty cycle of 3.5%, see Fig. 15. The average power in macro pulse is 1.2 W and 1.1 W. Applications with watt scale, high repetition rate THz radiation are carried out.

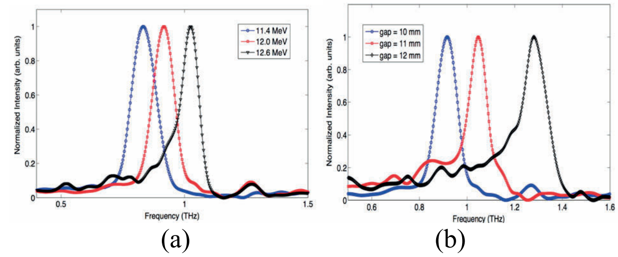

Figure 14: Measured THz spectra with different electron beam energies (a) and undulator gaps (b).

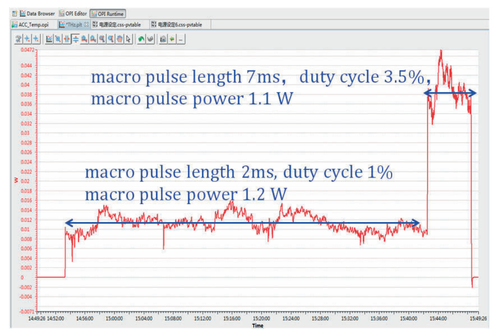

Figure 15: Measured THz power at different macro pulse.

CONCLUSIONS

Stable operation of the DC-SRF photoinjector and 2×9-cell SRF linac has been realized based on a series of improvements of drive laser, photocathode preparation, LLRF control system and diagnostic devices. Electron beam with energy of 8-25 MeV can be obtained with superconducting linac. The average beam current in macro pulses reached ~1 mA and was kept for long term operation at ~0.5 mA with the RF duty cycle up to 7% and repetition rate of 10 Hz. A series of applications have been carried with high repletion rate electron beam. A compact MHz repetition rate THz source was developed based on the DC-SRF photo-injector through velocity bunching. An average THz radiation power of mW level within macro pulses was experimentally detected, which is consistent with the calculation results considering the current low propagation efficiency of about 5.7×10^{-3}. MeV electron diffraction at MHz repetition rate has been demonstrated experimentally using electron pulses from a superconducting rf photoinjector, which shows the potential of high repetition rate pulses from the DC-SRF photoinjector for applications in UED. After improving the electron beam bunch energy to ~13 MeV with SRF linac and compressed with a Chicane structure, THz undulator radiation with an average power of 1 W has been achieved with gap-tuneable undulator. More applications with high repetition rate THz radiation are underway.

ISBN: 978-3-95450-199-1 doi:10.18429/JACoW-SAP2017-MOBH1

REFERENCES

[1] A. Arnold and J. Teichert, *Phys. Rev. ST Accel. Beams*, vol. 14 (2011), p. 024801.

[2] S. Belomestnykh, in *proc. FEL13*, New York, NY USA, 2013, p. 176.

[3] K. Zhao *et al.*, *Nucl. Instr. and Meth. A*, vol. 475 (2001), p. 564.

[4] J. Hao *et al.*, *Nucl. Instr. and Meth. A*, vol. 557 (2006) 138.

[5] Shengwen Quan, Feng Zhu, Jiankui Hao *et al.*, *Phys. Rev. ST Accel. Beams*, vol. 13 (2010), p. 042001.

[6] He Fei-Si, Hao Jian-Kui, Zhang Bao-Cheng, Zhao Kui, *Chinese Physics C*, vol. 32 (2008), p. 584.

[7] H. Zhang, J.-K. Hao, Lin Lin, K.X. Liu, F. Wang, B.C.Zhang, in *Proc. IPAC2011*, San Sebastián, Spain, 2011, p. 304.

[8] S.G. Anderson, P. Musumeci *et al.*, *Phys. Rev. ST Accel. Beams*, vol. 8 (2005), p. 014401.

[9] L. Serafini, M. Ferrario, in: S. Chattopadhyay *et al.* (Eds.), in *Proc. the AIP Conference* 581, *19th Advanced ICFA Beam Dynamics Workshop*, AIP, vol. 87, 2001.

[10] F. Kirchner, S. Lahme, F. Krausz and P Baum, *New J. Phys.*, vol. 15, p. 063021 (2013).

[11] M. Born and E. Wolf, "Principles of Optics: Electromagnetic Theory of Propagation, Interference and Diffraction of Light" (Oxford: Pergamon).